https://doi.org/10.5194/egusphere-2026-5162
Preprint. Discussion started: 12 November 2026
© Author(s) 2026. CC BY 4.0 License.

Aligning TIPMIP Models on a Common Global-Warming-Level Axis: A Standard Remapping Method for Multi-Model Comparison

Jakob Harteg[1,2,3], Colin Jones[4], Jonathan F. Donges[1,3], Manabu Abe[5], Patricia Cadule[6], Frederic Castruccio[7], Gokhan Danabasoglu[7], Friederike Fröb[8], Thomas L. Frölicher[9,10], Chuncheng Guo[11], Eike Köhn[12], Spencer Liddicoat[13], Anastasia Romanou[14,15], Yona Silvy[9,10], Tomas Torsvik[16], Klaus Wyser[17], Tokuta Yokohata[18], Tilo Ziehn[19], Ricarda Winkelmann[1,2,3], and Sina Loriani[1]

[1]Earth Resilience Science Unit, Potsdam Institute for Climate Impact Research, Member of the Leibniz Association, Telegrafenberg A 31, 14473 Potsdam, Germany
[2]Institute for Physics and Astronomy, University of Potsdam, Karl-Liebknecht-Str. 24/25, 14476 Potsdam-Golm, Germany
[3]Department Integrative Earth System Science, Max Planck Institute of Geoanthropology, Kahlaische Strasse 10, 07745 Jena, Germany
[4]National Centre for Atmospheric Science, University of Leeds, Leeds, LS2 9PH, UK
[5]Japan Agency for Marine-Earth Science and Technology, Yokohama, Japan
[6]LMD-IPSL, CNRS, Ecole normale supérieure/PSL, Sorbonne Université, Ecole Polytechnique, Paris, France
[7]National Science Foundation National Center for Atmospheric Research, Boulder, CO, USA
[8]Geophysical Institute, University of Bergen and Bjerknes Centre for Climate Research, Bergen, Norway
[9]Climate and Environmental Physics, Physics Institute, University of Bern, Switzerland
[10]Oeschger Centre for Climate Change Research, University of Bern, Switzerland
[11]Danish Meteorological Institute, Sankt Kjelds Plads 11, 2100 Copenhagen, Denmark
[12]LOCEAN-IPSL, Laboratoire d'Océanographie et du Climat: Expérimentations et Approches Numériques, Sorbonne Université-CNRS-IRD-MNHN, Paris, France
[13]Met Office Hadley Centre, FitzRoy Road, Exeter, EX1 3PB, United Kingdom
[14]NASA-Goddard Institute for Space Studies, New York, USA
[15]Department of Applied Physics and Applied Mathematics, Columbia University, New York, USA
[16]Geophysical Institute, University of Bergen, Bergen, Norway
[17]Swedish Meteorological and Hydrological Institute, Norrköping, Sweden
[18]National Institute for Environmental Studies, Tsukuba, Japan
[19]CSIRO Environment, Aspendale, Australia

Correspondence: Jakob Harteg (jakob.harteg@pik-potsdam.de)

Abstract. The Tipping Points Modelling Intercomparison Project (TIPMIP) samples common rates and levels of global warming (GWL) across physical, biophysical and biogeochemical domains, rather than a common calendar year or CO_2 level. In the Tier 1 experiments, emission-driven Earth system models (ESM) are forced by a constant CO_2-emission rate intended to yield 2 °C of warming per century. This ramp-up phase is followed by emission cessation (zero-emission runs) at selected GWLs, from which ramp-down runs are branched 50 years later using the negative of the ramp-up emission rate. A common rate of global warming is targeted in the ramp-up phase, but realised rates deviate from this target, particularly at higher levels of warming, and diverge further in the ramp-down phase, where the link between negative CO_2 emissions and global temperature is less established; as a result, equal calendar years do not correspond to equal GWLs across models. A standardised mapping

https://doi.org/10.5194/egusphere-2026-5162
Preprint. Discussion started: 12 November 2026
© Author(s) 2026. CC BY 4.0 License.



from model years to a temperature axis is therefore needed for diagnostics to be analysed and compared consistently as a function of GWL. We propose such a mapping here. We define GWL as the global-mean near-surface air temperature (GMSAT) anomaly relative to each model's own pre-industrial control, taken as a 31-year window centred on the branch year, the point at which the ramp-up run diverges from the pre-industrial control. The method maps any diagnostic from calendar time onto a common GWL axis in three steps: computing the warming anomaly, smoothing and enforcing monotonicity, and inverting the result to express any diagnostic against GWL at native resolution or on a shared grid. The inversion is applied to the ramp-up leg and to both Tier 1 ramp-down legs, from the zero emisison runs started at 2 and 4 °C GWL. Applying the method to nine available TIPMIP ESMs, we show the mapping is robust to its principal methodological choices, with baseline-window and smoothing-window sensitivities both under 0.1 °C, so results can be reported at 0.1 °C resolution regardless of these choices. We publish the resulting GWL axes for each model and leg as a versioned, provenance-stamped data product, together with an open-source Python implementation, so downstream analyses can share one common coordinate transformation rather than each constructing their own.

1 Introduction

The Tipping Points Modelling Intercomparison Project (TIPMIP; Winkelmann et al., 2025) assesses climate tipping-point risk in the Earth system; its Earth system model (ESM) Tier 1 protocol (Jones et al., 2026) is designed to bring Earth system models into a common global warming space. During the ramp-up experiment (`esm-up2p0`) each model is forced with a model-specific CO_2 emission rate, derived from its transient climate response to cumulative emissions (TCRE; Allen et al., 2009; Matthews et al., 2009), chosen to produce a global-warming rate of approximately 2 °C per century. In practice, however, models' realised warming rates deviate from this target, particularly at higher warming levels where the non-linearity of TCRE becomes significant; some models therefore warm substantially faster or slower than 2 °C per century, and the spread between them grows at higher levels of warming (Fig. 1, thin lines). Two models evaluated at the same calendar year are thus generally not in a comparable Earth-system state. The natural approach, and the one implied by the TIPMIP protocol's GWL-based experimental design, is to compare models at the same warming level rather than the same calendar year.

The protocol makes this possible in principle but not in practice. Jones et al. (2026) define GWL relative to each model's own pre-industrial control and use it to determine when a model branches from the ramp-up into its zero-emission runs, but they do not prescribe how to remap already-completed model output from calendar time onto a common temperature axis — the post-hoc step that any multi-model analysis requires. In the absence of a shared method, independent analyses will differ in their smoothing approach, baseline definition, and handling of edge cases, and their results will not be directly comparable. The remapping itself is conceptually simple: each model's time coordinate is replaced by a GWL coordinate, expressed as °C above that model's own pre-industrial baseline, after which any diagnostic is automatically aligned across models regardless of differences in calendar time or run length. What is missing is agreement on how the coordinate is constructed.

Existing GWL frameworks provide the ingredients for such an axis but none provides one ready-made for the TIPMIP ensemble. The dominant approach, implemented in ESMValTool (Swaminathan et al., 2022), defines warming anomalies

https://doi.org/10.5194/egusphere-2026-5162
Preprint. Discussion started: 12 November 2026
© Author(s) 2026. CC BY 4.0 License.

relative to a fixed 1850–1900 reference period, applies a 21-year running mean, and records the year at which each model first crosses a given temperature threshold, comparing variables in a time slice around that year. ISIMIP (Frieler et al., 2017) is closer to the TIPMIP approach: for ISIMIP2b and ISIMIP3b, crossing years are found from a 31-year running mean of the global-mean near-surface air temperature (GMSAT) relative to a per-model pre-industrial control rather than a fixed historical baseline, matching the protocol's 31-year window. These frameworks establish the ingredients this paper also relies on, a per-model control baseline and running-mean smoothing, but neither is built for TIPMIP's branching experimental design or for the continuous, per-model warming-level axis it requires.

Here we propose such an axis as a standard: a smooth, invertible coordinate that removes calendar-time ambiguity. We define GWL as the GMSAT anomaly relative to each model's own pre-industrial control, and construct the mapping through three documented steps (Sect. 2). We apply the same procedure to the ramp-up leg and to both ramp-down legs, enforcing a strictly-increasing monotonic axis on warming and a strictly-decreasing monotonic axis on cooling. We demonstrate the method on the nine currently available TIPMIP ESM Tier 1 models, and characterise which methodological choices affect the ramp-up result and which do not. We illustrate the transformation on a representative diagnostic, ocean mixed-layer depth (Fig. 3), and show how resampling onto the shared 0.02 °C grid exposes path dependence between ramp-up and ramp-down in mixed layer depth and sea-ice (Fig. 5). Because a separate mapping is required for each leg, we publish the resulting axes — 27 files for the nine models — as a versioned, provenance-stamped data product, so that comparability across downstream analyses is enabled by a shared mapping rather than left to each group to reproduce.

The zero-emission leg of the protocol is not mapped here. Because GMSAT does not evolve monotonically along it, the leg has no unique inverse map, so it cannot be resampled onto a common grid the way ramp-up and ramp-down are. Its forward map can still be computed directly, by applying Steps 1 and 2 to the ZEC leg's own GMSAT series, without the monotonicity-enforcement step, and relabelling each ZEC year with the resulting GWL value using `relabel_to_gwl`. The trajectory this produces can then be plotted alongside the mapped ramp-up and ramp-down legs on the same axis. Treating it as its own mapped axis in the published product, and placing all three legs on a single hysteresis diagram, we leave to future work.

2 Proposed method

The method proceeds in three steps, applied identically to every model and protocol leg:

1. **Step 1 (anomaly):** subtract each model's own baseline (a 31-year `esm-piControl` mean centred on the branch year) from the raw GMSAT series of each leg.

2. **Step 2 (smoothing and monotonicity):** apply a 31-year centred running mean, then enforce monotonicity via isotonic regression (PAVA), giving the smooth, monotone axis `GWL(t)`.

3. **Step 3 (relabelling and resampling):** invert `GWL(t)` to express any diagnostic against GWL, either by relabelling at native resolution or resampling onto a common grid.

https://doi.org/10.5194/egusphere-2026-5162
Preprint. Discussion started: 12 November 2026
© Author(s) 2026. CC BY 4.0 License.

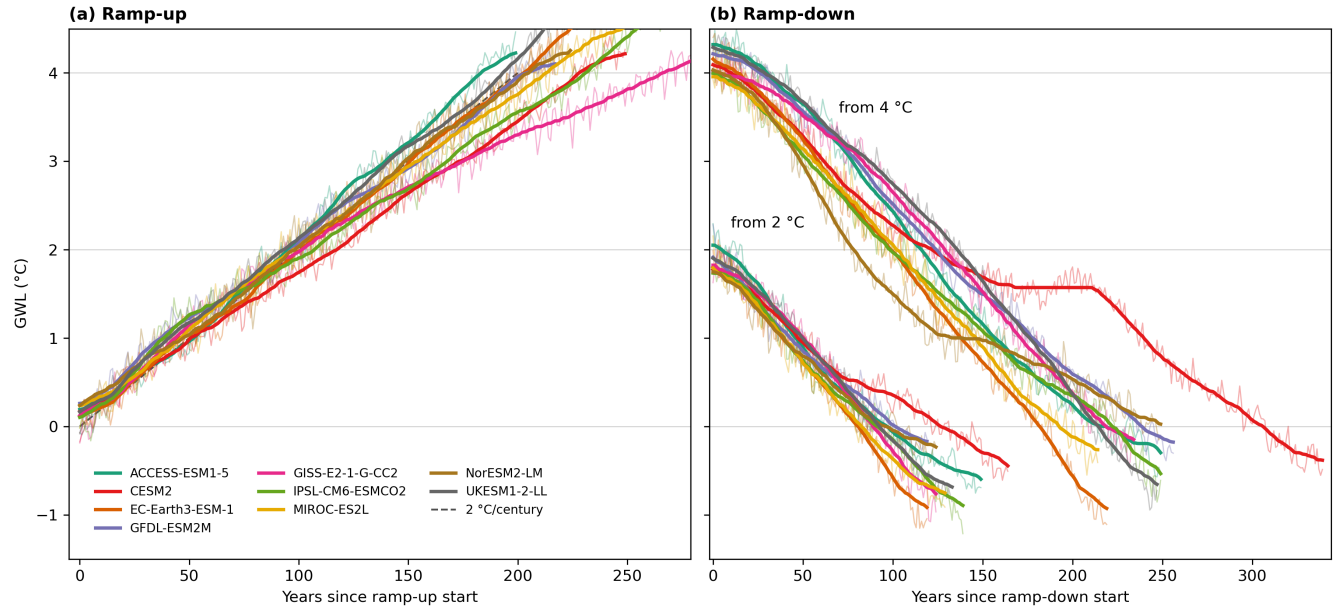


Figure 1. Monotone global-warming-level (GWL) axes for the ramp-up and ramp-down legs. GMSAT anomaly for each of the nine Tier 1 TIPMIP ESMs, plotted against years since the start of the respective leg: (a) ramp-up (`esm-up2p0`); (b) ramp-down after 50 years of zero-emissions started at 2 and 4 °C GWL (both branches overlaid). Thin lines show the days-in-month-weighted annual-mean anomaly; thick lines show the monotone axis used for re-indexing (31-year centred running mean with edge-shortened windows at leg ends, then isotonic regression; increasing on ramp-up, decreasing on ramp-down; Sect. 2). Anomalies are referenced to each model's own `esm-piControl` baseline (Fig. 2).

Each step is described below and implemented as a documented function in the accompanying software. A separate mapping product is built for the ramp-up leg and for each ramp-down branch (from 2 and 4 °C GWL after 50 years of zero-emissions); the ramp-down is treated in Sect. 2.2.

2.1 Algorithm and ramp-up mapping

2.1.1 Step 1: Anomaly computation

We build the temperature axis from near-surface air temperature. In CMIP this field is `tas`; we define global-mean near-surface air temperature (GMSAT) as the area-weighted global mean of `tas`, reduced to a days-in-month-weighted annual mean. We compute GMSAT for the ramp-up (`esm-up2p0`), the ramp-down legs `esm-up2p0-gwl2p0-50y-dn2p0` and `esm-up2p0-gwl4p0-50y-dn2p0`, and `esm-piControl` runs using CDO's `fldmean`, which weights each grid cell by the area derived from its grid description.

We define the baseline as the mean GMSAT of each model's own `esm-piControl` run over a 31-year window centred on the ramp-up branch year (Fig. 2; the branch year is decoded from `branch_time_in_parent` and `parent_time_units`

https://doi.org/10.5194/egusphere-2026-5162
Preprint. Discussion started: 12 November 2026
© Author(s) 2026. CC BY 4.0 License.

with `cftime`, or supplied by the modelling group where archived metadata are incomplete; see Appendix A). This matches the diagnostic window in the protocol for branch-off at specified GWL (Jones et al., 2026). The same scalar baseline is subtracted from ramp-up and ramp-down GMSAT, so each model has one pre-industrial reference shared across legs. For ACCESS-ESM1-5, EC-Earth3-ESM-1, GFDL-ESM2M, GISS-E2-1-G-CC2, and NorESM2-LM, whose branch years fall at the start of the staged `esm-piControl` record, a centred window is not possible and we use the first 31 years (trailing window) instead. As a check on the window baseline we also compute the full-run `esm-piControl` mean for every model and compare the two (Sect. 2.3; Fig. 6; Table A1).

Subtracting the baseline from each leg's GMSAT series gives that leg's warming anomaly relative to the model's own pre-industrial state, on the model's native calendar.

2.1.2 Step 2: Smoothing and monotonicity

We apply a 31-year centred running mean to each leg's anomaly series. Where a full centred window would extend past the start or end of the leg, the window is truncated to the available years. The outer ∼15 years of each leg use shorter effective windows and are therefore less smoothed than the interior. Smoothing is necessary because interannual variability of order 0.1–0.2 °C is comparable to roughly a decade of forced trend at the target warming rate of 2 °C per century (Jones et al., 2026). Without it, a single anomalously warm year can render the series locally non-monotone and make the subsequent inversion multi-valued or noisy. The 31-year window matches the protocol's own diagnostic window (Jones et al., 2026), keeping the smoothed axis consistent with how GWL crossings were defined during the simulations. Smoothing is applied only to the axis-defining variable, the GMSAT anomaly. Diagnostic variables such as mixed-layer depth or sea-ice concentration are carried through unsmoothed, so that genuine abrupt changes in the variables of interest are not artificially blurred.

We then apply isotonic regression via the pool-adjacent-violators algorithm (PAVA; Ayer et al., 1955; Barlow et al., 1972), which merges (pools) any adjacent points that violate monotonicity into their shared average until the sequence is monotone, to enforce monotonicity along each leg: non-decreasing on ramp-up and non-increasing on ramp-down. Where PAVA removes a local violation it may introduce short flat segments; if the smoothed series is already strictly monotone, this step is the identity. We separately track how much this step moves the already-smoothed series in the diagnostic `mono_max`, in °C, where a near-zero value means the axis was already monotone (stored as `monotonization_max` in the mapping products). See Sect. 2.3 for details and Table A2 for per-model values. The result is the smooth, monotone temperature axis used for inversion, the thick lines in Fig. 1.

2.1.3 Step 3: Relabelling and resampling

Step 3 works one leg at a time: ramp-up, or one of the two ramp-down branches, using that leg's own mapping product. Within a leg, a diagnostic can be expressed against GWL two ways: *relabelling*, which applies the forward map `GWL(t)` directly to the diagnostic's own time points, or *resampling*, which uses the inverse map `t(GWL)` to interpolate the diagnostic onto a common grid. We explain both below.

https://doi.org/10.5194/egusphere-2026-5162
Preprint. Discussion started: 12 November 2026
© Author(s) 2026. CC BY 4.0 License.

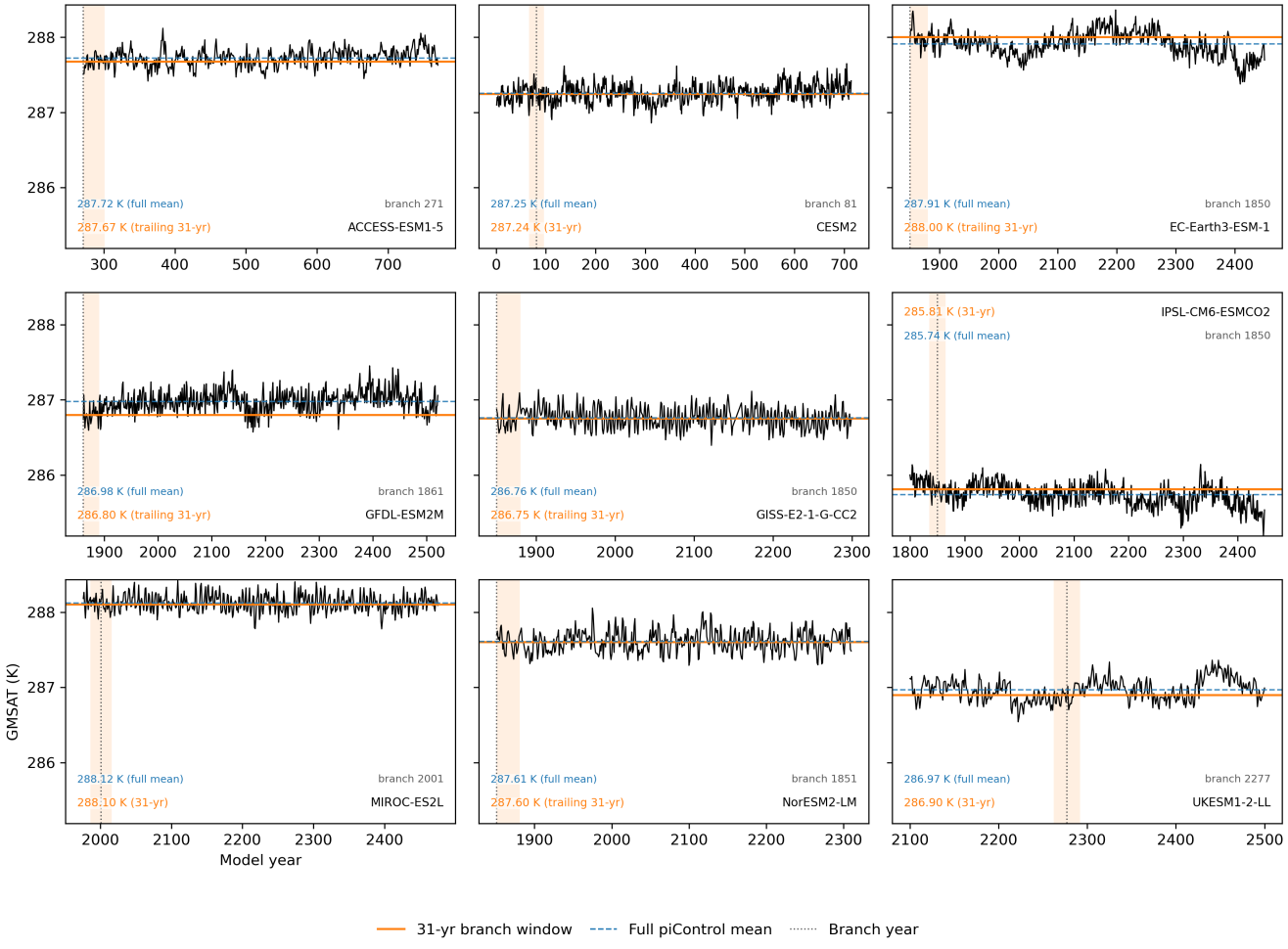


Figure 2. `esm-piControl` GMSAT and baseline definitions. Annual-mean emission-driven pre-industrial control (`esm-piControl`) GMSAT for each model (black). The solid orange line is the mean over a 31-year window, centred on the ramp-up branch year (shaded) where possible. For ACCESS-ESM1-5, EC-Earth3-ESM-1, GFDL-ESM2M, GISS-E2-1-G-CC2, and NorESM2-LM, whose branch years fall at the very start of the staged `esm-piControl` record, a trailing window is used instead. The dashed blue line is the full `esm-piControl` mean. The dotted vertical line marks the branch year.

Relabelling the time-axis (Fig. 3). The temperature axis itself is built at annual resolution: one GWL value per calendar year, from the 31-year-smoothed, monotone GMSAT series (Step 2). The diagnostic being remapped can be supplied at any native resolution (annual, monthly, or finer) and each of its time steps is assigned a GWL by linear interpolation in calendar time between the two nearest annual anchors (time coordinates must be numeric calendar years, not datetime objects); sub-annual timestamps therefore receive sub-annual GWL values, not one held constant across the year. This is the appropriate form for inspecting or plotting a single model's diagnostic against warming level on a single leg, where preserving the original

https://doi.org/10.5194/egusphere-2026-5162
Preprint. Discussion started: 12 November 2026
© Author(s) 2026. CC BY 4.0 License.

resolution matters and no cross-model alignment is required. Fig. 3 demonstrates this on global-mean annual-maximum mixed-layer depth, relabelling all nine models from their native calendar axes onto GWL for the ramp-up leg: the same feature can then be read and visually compared at the warming level where it occurs in each model, though the underlying points are not yet aligned onto matching grid values across models (Fig. 4).

Because relabelling does not resample the diagnostic onto a common grid, points are unevenly spaced in GWL. Time series operations such as smoothing or abrupt-shift detection should therefore be performed on the diagnostic's native calendar-time axis; use the mapping only to attach a GWL value to features already identified there.

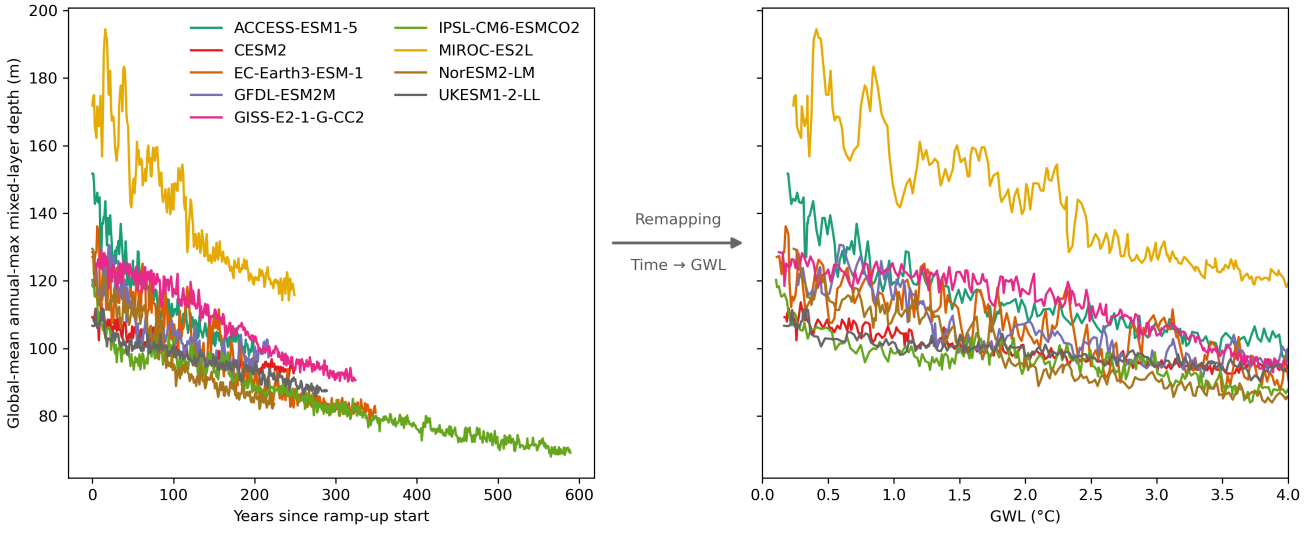


Figure 3. The same diagnostic before and after temperature-axis remapping. Global-mean annual-maximum ocean mixed-layer depth (`mlotst`) for all nine models, (left) on each model's native calendar-year axis and (right) relabelled with each year's GWL via the forward transform `GWL(t)` (Step 3, relabelling). On the native time axis the models span different run lengths and warming rates, so a given feature falls at a different year in each model; on the GWL axis the same curves are expressed against warming level and can be compared where each feature occurs. This panel uses continuous relabelling, not resampling onto the shared 0.02 °C grid — native annual resolution is preserved and nothing is interpolated beyond assigning each timestep its GWL. The diagnostic is unsmoothed — only the temperature axis is smoothed (Step 2), never the variable remapped through it — and values are not extrapolated beyond each model's realised warming range on the forward axis. Panel (b) is displayed for 0–4 °C to match the ramp-up resampling grid; curves for models that warm past 4 °C are truncated at the axis limit (full axis in Fig. 1a). The global mean is area-weighted by $\cos(\text{latitude})$, an approximation adopted because no ocean cell-area field (`areacello`) was staged for these curvilinear grids.

Resampling onto a common grid (Fig. 4). Use this when comparing models or legs value-by-value (ensemble statistics, differencing at fixed GWL). Step 2 can leave short flat segments where PAVA merges nearby years; we nudge these to a strictly increasing sequence (by far less than 0.02 °C) so inversion is unique. We then invert the monotone axis by monotone cubic (PCHIP) interpolation, which, unlike a standard cubic spline, preserves monotonicity between input points and so avoids

https://doi.org/10.5194/egusphere-2026-5162
Preprint. Discussion started: 12 November 2026
© Author(s) 2026. CC BY 4.0 License.

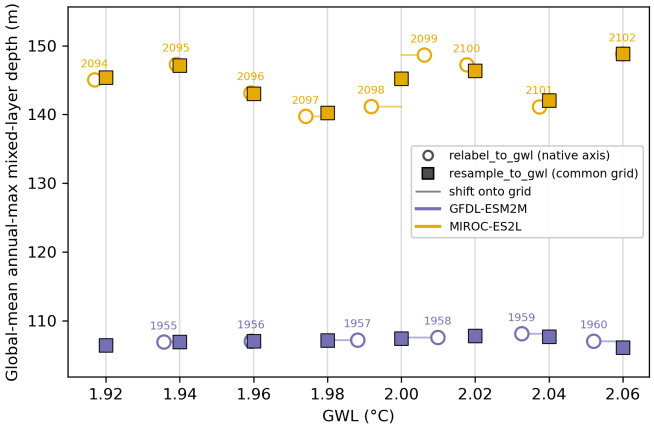


Figure 4. Relabelling versus resampling, close up. Global-mean annual-maximum mixed-layer depth for two models (GFDL-ESM2M, purple; MIROC-ES2L, gold) over a narrow GWL range, illustrating the two forms of the mapping described in Step 3. Open circles show `relabel_to_gwl`: each model's native annual value, plotted at that year's own continuous GWL (calendar years labelled). Filled squares show `resample_to_gwl`: the same diagnostic resampled onto the shared 0.02 °C grid, obtained by inverting the temperature axis to the fractional year at each grid point and linearly interpolating the diagnostic there. The connecting line joins each native point to its resampled counterpart, showing both the shift onto a common grid position and the accompanying change in value introduced by interpolation. Once resampled, both models' diagnostics sit on identical GWL grid points, the form required for value-by-value comparison across models.

introducing spurious oscillation into the inverted map, to obtain the fractional model year at each GWL, and resample the diagnostic onto a fixed grid: 0 °C to +4 °C for ramp-up, and −2 °C to +5 °C for ramp-down, both at 0.02 °C spacing (201 and 351 points). The wider bounds used for the ramp-down legs allow for a possible temperature drift in the 50 years of zero-emission run before the negative emission (cooling) run starts, and also allows the sub-baseline cooling trajectory to be inspected for hysteresis. The 0–4 °C points are identical across legs, enabling the point-by-point differencing in Fig. 5. On ramp-up, only the inverse map on 0–4 °C is stored, matching the Tier 1 grid used throughout; any submitted data beyond 4 °C is retained by relabelling but not included in the resampled product. Values are NaN beyond each model's realised range. The diagnostic is linearly interpolated in time at the inverted year; sub-annual input improves precision where abrupt timing matters.

In both representations the coordinate is renamed from time to `gwl` with units of °C, making explicit that it no longer represents calendar time. The two forms are consistent by construction: the gridded form is the continuous axis evaluated on a fixed grid.

2.2 Ramp-down mapping

The Tier 1 protocol continues each ramp-up simulation into a zero-emission run, branched off at 2 °C and 4 °C GWL. Fifty years into each zero-emission run, a ramp-down experiment is branched, forced by negative CO_2 emissions: the exact negative of the ramp-up's positive emissions, i.e. CO_2 removed from the model atmosphere. While the global cooling rate in the ramp-

https://doi.org/10.5194/egusphere-2026-5162
Preprint. Discussion started: 12 November 2026
© Author(s) 2026. CC BY 4.0 License.

down is an emergent property of each model, our expectation is it will be approximately $-2\,^{\circ}$C/century. We construct one decreasing monotone axis per ramp-down simulation, using the same three steps and the same `esm-piControl` baseline as for ramp-up. The resulting mapping products are published alongside the ramp-up files; users select the leg with the `leg` argument in the software (e.g. `ramp-down-2c`, `ramp-down-4c`).

Fig. 1b shows the ramp-down GMSAT anomaly and monotone axis for both branches overlaid in GWL–time space. The branch from 4 °C spans much of the 0–4 °C interval on the cooling leg (over the staged run length) and is the natural counterpart to ramp-up for hysteresis-style comparisons; the branch from 2 °C spans a narrower GWL range, but is the natural counterpart for hysteresis at that branch point. On ramp-up, the monotone axis often begins slightly above 0 °C even when the raw annual anomaly at the branch instant is near zero or negative. At the leg start the running mean uses a shortened window over the earliest years of warming, so the first axis value reflects early post-branch warming rather than the unsmoothed anomaly at a single calendar year. Consequently `t(0)` is undefined on the monotone axis and remapped diagnostics are not available below each model's realised minimum GWL on that leg. The resampling grid for ramp-up begins at 0 °C, but values below a model's realised minimum remain NaN.

Fig. 5 illustrates the gridded form (Step 3) across three regional diagnostics: Subpolar Gyre mixed-layer depth for GFDL-ESM2M, and Arctic and Antarctic sea-ice volume for UKESM1-2-LL, each resampled onto the shared 0.02 °C grid with the ramp-up mapping and the ramp-down-from-4 °C mapping. Resampling both legs onto the same grid lets them be compared directly at fixed GWL, as shown here; the models are chosen for clarity, not as representative of the ensemble.

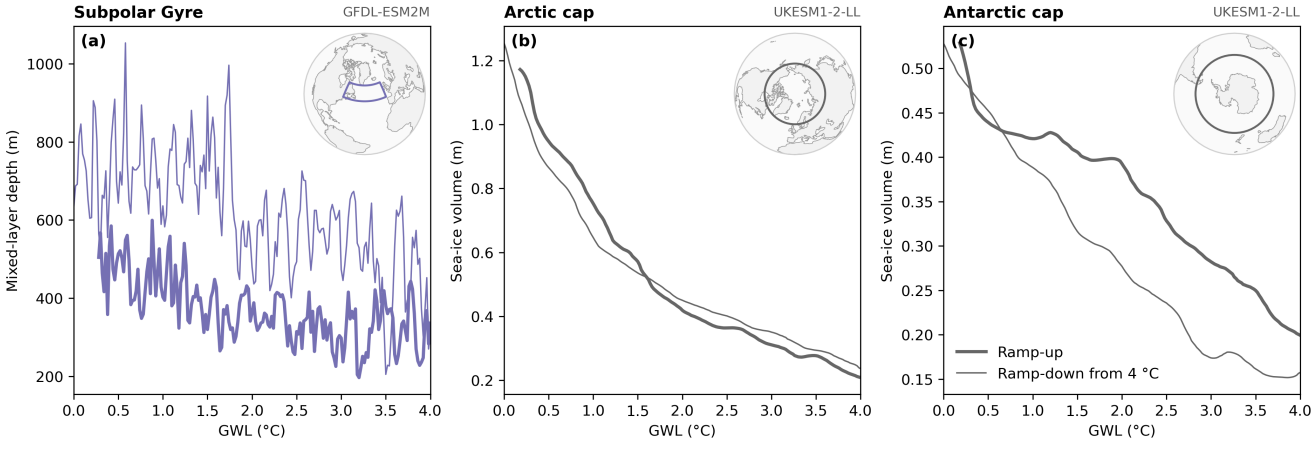


Figure 5. Path dependence after resampling onto the common GWL axis, shown for three regional diagnostics. (a) Subpolar Gyre (45–60 °N, 70–10 °W) annual-maximum mixed-layer depth for GFDL-ESM2M; (b) Arctic (≥60 °N) and (c) Antarctic (≤50 °S) annual-mean sea-ice volume per area for UKESM1-2-LL (polar series smoothed with a 6-yr Gaussian filter). All series are resampled with `resample_to_gwl` onto the shared 0.02 °C grid (0–4 °C), using the ramp-up mapping (thick line) and the ramp-down-from-4 °C mapping (thin line). The Arctic shows little separation between legs; the Antarctic shows a persistent, approximately constant offset. The sign and magnitude of panel (a)'s leg separation vary across models (including in direction) and are not interpreted here.

https://doi.org/10.5194/egusphere-2026-5162
Preprint. Discussion started: 12 November 2026
© Author(s) 2026. CC BY 4.0 License.

The zero-emission leg is not treated here as its own mapped axis: GMSAT changes over this part of the protocol according to each model's zero-emissions commitment (Jones et al., 2019), so it is not a simple monotone inversion problem. Placing the ramp-up, zero-emission, and ramp-down on a single continuous hysteresis diagram remains for future work.

2.3 Robustness and diagnostics

The mapping depends on a small number of methodological choices; here we characterise how much each choice affects our results. For the ramp-up leg we examine two choices — the baseline definition and the smoothing-window width — and we report the monotonicity correction as a per-model diagnostic. The ramp-down legs use the same Step 1–2 pipeline (identical `esm-piControl` baseline inherited from the ramp-up mapping product, 31-year centred running mean, decreasing isotonic regression). Because the baseline and smoothing choices are fixed across legs, we do not repeat the baseline or window sweeps for ramp-down; the leg-specific check is `mono_max`, which flags plateaus or reversals on the decreasing GWL axis. Per-model `mono_max` for all three legs is given in Table A2.

Baseline (ramp-up). A branch year is available for every model in the ensemble, so the adopted baseline is uniquely determined. As a check on the branch-year-centred window adopted in Step 1, we also computed the full-run `esm-piControl` mean. Because `esm-piControl` drift is small for every model, the two agree to within 0.089 K for eight of the nine models (Fig. 6; Table A1), below the 0.1 °C resolution at which we report GWL; for GFDL-ESM2M, whose branch year falls at the start of a 661-year control, the difference is 0.182 K. The drift itself serves as a quality control on the window baseline: fitting a linear trend to each control's GMSAT (Fig. 6; Table A1) confirms the drift is small in every model — at most ∼0.04 °C/century — so a larger difference reflects low-frequency variability in the control record rather than uncertainty in the adopted baseline, which is tied to the branch instant by construction.

Five models use a trailing 31-year branch window (Step 1): ACCESS-ESM1-5, EC-Earth3-ESM-1, GFDL-ESM2M, GISS-E2-1-G-CC2, and NorESM2-LM. A trailing window shifts the midpoint of the baseline period by about 15 years relative to a centred window. With low `esm-piControl` drift, that shift introduces only a small systematic offset in the reference temperature: at most about 0.004 °C, given drift magnitudes of 0.026 °C/century or less for these five models. These values are negligible at our reporting resolution.

Smoothing window (ramp-up). Varying the smoothing-window length between 21, 31, and 41 years shifts the year assigned to a fixed GWL by at most about 3.4 years across all models — roughly 0.07 °C-equivalent at the nominal 2 °C/century rate. We retain the protocol's 31-year window as the fixed choice for all legs.

Monotonicity (`mono_max`). The pool-adjacent-violators step of Step 2 moves the smoothed axis by at most 0.003 °C on ramp-up. On the ramp-down legs, `mono_max` is 0.007 °C or smaller for eight of the nine models, and 0.055 °C for CESM2, 4 °C branch, reflecting an extended stretch where the model's raw annual cooling departs from a steady decrease (Sect. 4). All values remain below our 0.1 °C reporting resolution, though the margin for CESM2's 4 °C branch is smaller than for the rest of the ensemble. Where the monotonicity step introduces short flat segments, the small perturbation described in Step 3 ensures the subsequent inversion remains well-posed. For ramp-down, `mono_max` is the primary leg-specific diagnostic: it

https://doi.org/10.5194/egusphere-2026-5162
Preprint. Discussion started: 12 November 2026
© Author(s) 2026. CC BY 4.0 License.

tests whether the cooling trajectory is sufficiently monotone for a well-posed time→GWL inversion without repeating the baseline or window analyses, which are shared with ramp-up by construction.

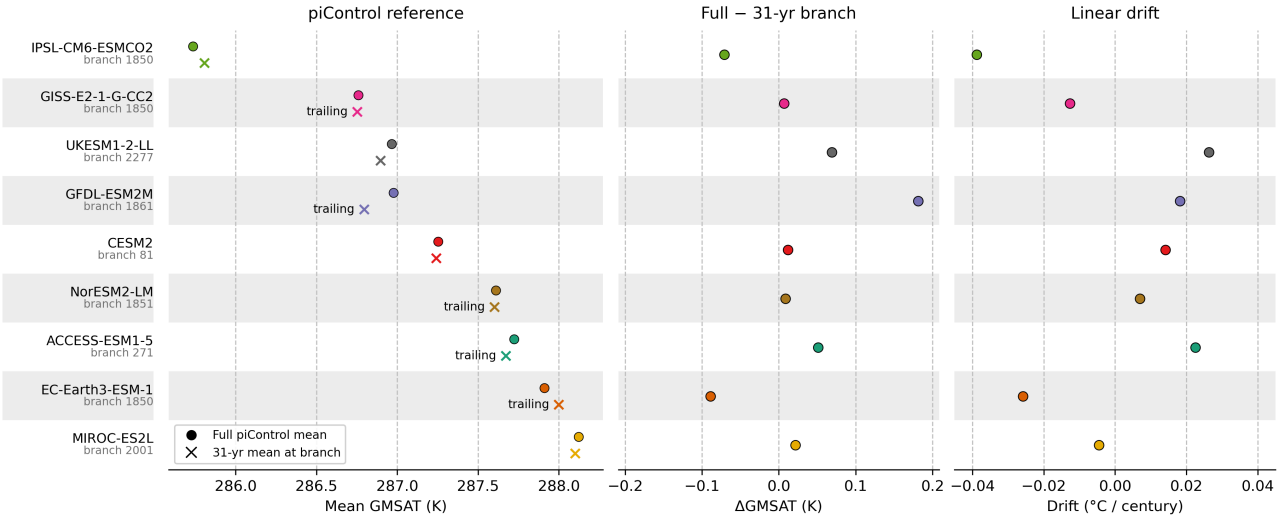


Figure 6. Baseline check: branch-year window vs. full `esm-piControl` mean. Comparison of the baseline adopted in Step 1 with the full-run control mean, for all nine models, sorted by `esm-piControl` reference temperature. Left panel: the 31-year mean centred on the branch year (cross, the adopted baseline; labelled "trailing" for ACCESS-ESM1-5, EC-Earth3-ESM-1, GFDL-ESM2M, GISS-E2-1-G-CC2, and NorESM2-LM, whose branch years fall at the start of the staged `esm-piControl` record) and the full-run `esm-piControl` mean (circle, reported as a check), in K. Middle panel: their difference (full − window); the two agree to within 0.09 K for eight of the nine models, and to 0.182 K for GFDL-ESM2M. Right panel: linear drift of the full `esm-piControl` run, in °C per century.

3 Code and data product

The method is distributed as the open-source Python package `tipmip-gwl` (Harteg, 2026a), which implements each step of the mapping and computes the diagnostics reported here, including the `esm-piControl` drift and the robustness comparisons. Global-mean series are formed with `cdo fldmean` and reduced to a days-in-month-weighted annual mean for the mapping. All figures and tables in this paper are reproduced from the same inputs by a single driver script. The package enforces one hard requirement — a matching `esm-piControl tas` file, without which no baseline can be formed — and records other provenance irregularities as warnings in the output rather than rejecting the model, so any such issue stays explicit and traceable while usable models are still processed.

Because the mapping is a deterministic function of a model's ramp-up/ramp-down and `esm-piControl` temperatures, it needs to be computed only once per model per leg. We publish the result as a data product at https://github.com/tipmip-methods/tipmip-gwl so that downstream analyses can adopt a common mapping rather than each reconstructing one. For each model the

https://doi.org/10.5194/egusphere-2026-5162
Preprint. Discussion started: 12 November 2026
© Author(s) 2026. CC BY 4.0 License.

product provides the temperature axis in both forms described in Step 3: the forward map `GWL(t)`, which relabels a diagnostic at its native resolution, and the inverse map `t(GWL)` on a fixed grid in 0.02 °C steps (0 °C to +4 °C for ramp-up, −2 °C to +5 °C for ramp-down) which resamples it for cross-model and cross-leg comparison. Each file also carries the per-model diagnostics (Table A1; Table A2), follows CF metadata conventions, and is loadable like the rest of the archive. The product ships the coordinate transform only, not pre-remapped diagnostic variables: users apply the axis to whatever variable they need, which keeps it a bounded coordinate product rather than an open-ended data-production effort.

The product is versioned. Each file records the `tracking_ids` of its input files, the version of the code that produced it, and a mapping version, so that a downstream analysis can reference an exact version and so that the product can be regenerated as models are added or their staged data corrected. Version 1.0 covers all nine currently staged models (Harteg, 2026a); the latest release is (Harteg, 2026b).

4 Discussion

TIPMIP exists to assess the risk of Earth system tipping points, self-amplifying feedbacks in the ice sheets, the AMOC, permafrost, and forests, among other systems, that could drive non-linear, abrupt, and potentially irreversible changes (Winkelmann et al., 2025). Its experiment protocol departs from standard practice: rather than aligning models by a common CO_2 concentration or emissions pathway, as in the SSP and 1pctCO_2 experiments, it aligns them by the rate and level of global warming. This matters because models differ in how much warming a given amount of CO_2 produces; the same forcing scenario can leave two models at very different temperatures. The primary driver of change and impacts for both natural systems and human societies is warming itself, and the associated climate and ecosystem responses to that warming; CO_2 concentration also has a direct impact on some Earth-system components (e.g. terrestrial and ocean ecosystems), but this is generally smaller than the effect of warming. This is reflected in how climate policy is formulated: targets are set in temperature terms, 1.5 °C or 2 °C, with allowable cumulative CO_2 emissions calculated as those consistent with a defined probability of remaining below the target, rather than policy being framed around atmospheric CO_2 concentration directly. Comparing models at equal warming levels is therefore both physically and practically the preferred approach for assessing tipping risks (Jones et al., 2026). Making that comparison requires knowing which warming level each model has actually reached at each point in its simulation, something the protocol defines operationally but does not, by itself, provide a way to compute from model output. The mapping presented here supplies that missing piece: a standardised, versioned warming-level axis for every model and protocol leg, so that TIPMIP's multi-model assessment of tipping risk is built on results genuinely comparable at equal warming, not just nominally aligned by experiment design.

The mapping presented here covers both the ramp-up leg and the two Tier 1 ramp-down legs. Resampling a diagnostic onto the shared GWL grid for both a warming and a cooling leg, as demonstrated for mixed-layer depth in Fig. 5, allows reversibility and path-dependence at fixed GWL to be read directly. The zero-emission phase is a different case, since temperature is not strictly constant along it and models depart from their branching GWL according to their zero emissions commitment (ZEC; Jones et al., 2019); placing all three legs on a single hysteresis diagram remains for future work. The method's requirements

https://doi.org/10.5194/egusphere-2026-5162
Preprint. Discussion started: 12 November 2026
© Author(s) 2026. CC BY 4.0 License.

are otherwise minimal: a piControl-relative GMSAT series and a leg designed to warm or cool monotonically. This makes it extensible to other ramp rates and branch points as the TIPMIP protocol develops (Jones et al., 2026), and to the offline, domain-specific models (ice-, ocean-, and land-only) that TIPMIP ESM output is used to force: because the axis is built entirely from the driving ESM's own temperature variable (`tas`), the published mapping can relabel or resample an offline model's output directly, provided its calendar stays synchronised with the driving ESM's.

The published grid is sampled at 0.02 °C, but methodological uncertainty means a reported GWL value should be rounded to the nearest 0.1 °C; differences finer than this are not meaningful, though the finer grid remains useful for downstream computation. Relabelling (`relabel_to_gwl`) assigns each time step its own GWL without resampling, so the resulting points are unevenly spaced in GWL; time series methods that assume even spacing (e.g. smoothing, abrupt-shift detection) should not be applied directly to a relabelled series. Such analysis should instead be performed on an evenly-spaced representation of the data, either the diagnostic's native calendar-time axis or the resampled GWL grid (`resample_to_gwl`), with relabelling reserved for attaching a GWL value to features already identified there, or for inspecting a single model's diagnostic against warming level. Resampling onto the GWL grid has the added property that grid spacing is even in GWL but not in real time: where a model's realised rate departs from the nominal ∼2 °C/century, grid points no longer correspond one-to-one with calendar years, so slow periods are oversampled relative to real time, e.g. CESM2's 4 °C ramp-down branch, which plateaus near GWL = 1.56 °C for roughly 130 years (Fig. 1b), is an extreme case.

As the TIPMIP ensemble grows, the same procedure applies unchanged; the per-model diagnostics reported here (Tables A1, A2) provide a built-in check that this robustness continues to hold, since a future model or leg with substantially larger `esm-piControl` drift or non-monotonic warming would be flagged directly by a larger `mono_max` or $|\Delta\mathrm{ref}|$, rather than silently violating the assumptions the robustness analysis rests on.

The value of this mapping lies in what it enables for TIPMIP's central question: whether and where tipping points are likely to be crossed as warming progresses. Tipping thresholds are hypothesised at warming levels, not calendar years or CO_2 concentrations, so comparing tipping risk across models presupposes a warming-level axis that is itself reliable. By fixing that axis as a shared, versioned standard, this mapping lets subsequent TIPMIP analyses of ice sheets, the AMOC, permafrost, and forests build on a common notion of "how much warming," rather than each study settling that question for itself.

Code and data availability. The `tipmip-gwl` software and the published GWL coordinate products (27 NetCDF files, mapping version v1.0, in the repository's `mapping/` directory) are openly available at https://github.com/tipmip-methods/tipmip-gwl and archived on Zenodo (version 1.1 used in this paper: https://doi.org/10.5281/zenodo.23263429 (Harteg, 2026a); latest version: https://doi.org/10.5281/zenodo.22084351, (Harteg, 2026b)). Each file holds the derived calendar-year ↔ GWL mapping for one model and leg (nine Tier-1 models × three legs); raw TIPMIP fields are not redistributed.

https://doi.org/10.5194/egusphere-2026-5162
Preprint. Discussion started: 12 November 2026
© Author(s) 2026. CC BY 4.0 License.

Author contributions. JH wrote the paper, developed the software and mapping products, and performed the analysis. CJ, JFD, SpL, and SL contributed text and provided extensive comments throughout. RW initiated and leads TIPMIP. Modelling-group co-authors AR, CG, FC, FF, TT, GD, KW, PC, EK, MA, YS, TY, and TZ contributed data. All authors reviewed and approved the final manuscript.

Competing interests. At least one of the (co-)authors is a member of the editorial board of Geoscientific Model Development.

Acknowledgements. This is ClimTip contribution #183; the ClimTip project has received funding from the European Union's Horizon Europe research and innovation programme under grant agreement No. 101137601: Funded by the European Union. Views and opinions expressed are however those of the author(s) only and do not necessarily reflect those of the European Union or the European Climate, Infrastructure and Environment Executive Agency (CINEA). Neither the European Union nor the granting authority can be held responsible for them.

We acknowledge the Tipping Points Modelling Intercomparison Project (TIPMIP) and its participants for producing and publishing their simulation data. We thank the Max-Planck Institute of Geoanthropology (MPI-GEA) and the Potsdam Institute for Climate Impact Research (PIK) for coordinating TIPMIP and providing the infrastructure necessary to advance the project. We also thank the many people and institutions behind the Coupled Model Intercomparison Project (CMIP) and the Earth System Grid Federation (ESGF) for their guidance and support of initiatives such as TIPMIP. This is TIPMIP contribution #05.

CJ acknowledges TipESM "Exploring Tipping Points and Their Impacts Using Earth System Models" funded by the European Union; Grant Agreement: 101137673, and the UKRI Guarantee Agreements: 10090271, 10110109, 10121766, 10103098.

CJ acknowledges OptimESM "Optimal High Resolution Earth System Models for Exploring Future Climate Changes" funded by the European Union; Grant Agreement: 101081193 and the UKRI Guarantee Agreements: 10043072, 10041076, 10040511, 10038604.

TZ receives funding from the Australian Government through the National Environmental Science Program.

TY was supported by the Program for the Advanced Studies of Climate Change Projection (SENTAN, Grant JPMXD0722681344) from the Ministry of Education, Culture, Sports, Science and Technology of Japan.

MA was supported by the Program for the Advanced Studies of Climate Change Projection (SENTAN, Grant JPMXD0722681344) from the Ministry of Education, Culture, Sports, Science and Technology of Japan.

AR was supported with funding from NASA-IMVI.

C.G. acknowledges OptimESM, which has received funding from the European Union's Horizon Europe research and innovation programme under grant agreement No. 101081193, and TipESM "Exploring Tipping Points and Their Impacts Using Earth System Models". TipESM is funded by the European Union. Grant Agreement number: 101137673.

KW acknowledges TipESM "Exploring Tipping Points and Their Impacts Using Earth System Models" and OptimESM "Optimal High Resolution Earth System Models for Exploring Future Climate Changes", funded by the European Union (Grant Agreements 101137673 and 101081193).

Some of the computational resources for EC-Earth were provided by the National Academic Infrastructure for Supercomputing in Sweden (NAISS), funded by the Swedish Research Council.

The US National Science Foundation National Center for Atmospheric Research (NSF NCAR) is a major facility sponsored by the US NSF under Cooperative Agreement 1852977. GD and FC were partly supported by the ImPACTS Project.

https://doi.org/10.5194/egusphere-2026-5162
Preprint. Discussion started: 12 November 2026
© Author(s) 2026. CC BY 4.0 License.

We used AI coding and writing assistants (Anthropic Claude, Cursor, Composer 2.5) to help develop the software and improve manuscript readability. All scientific content, interpretations, and results were written and verified by the authors, who take full responsibility for the paper and code.

Financial support. The article processing charges for this open-access publication were covered by the Potsdam Institute for Climate Impact Research (PIK).

https://doi.org/10.5194/egusphere-2026-5162
Preprint. Discussion started: 12 November 2026
© Author(s) 2026. CC BY 4.0 License.

References

Allen, M. R., Frame, D. J., Huntingford, C., Jones, C. D., Lowe, J. A., Meinshausen, M., and Meinshausen, N.: Warming caused by cumulative carbon emissions towards the trillionth tonne, Nature, 458, 1163–1166, https://doi.org/10.1038/nature08019, 2009.

Ayer, M., Brunk, H. D., Ewing, G. M., Reid, W. T., and Silverman, E.: An empirical distribution function for sampling with incomplete information, The Annals of Mathematical Statistics, 26, 641–647, https://doi.org/10.1214/aoms/1177728423, 1955.

Barlow, R. E., Bartholomew, D. J., Bremner, J. M., and Brunk, H. D.: Statistical Inference under Order Restrictions: The Theory and Application of Isotonic Regression, John Wiley & Sons, London and New York, ISBN 0471049700, 1972.

Frieler, K., Lange, S., Piontek, F., et al.: Assessing the impacts of 1.5 °C global warming – simulation protocol of the Inter-Sectoral Impact Model Intercomparison Project (ISIMIP2b), Geoscientific Model Development, 10, 4321–4345, https://doi.org/10.5194/gmd-10-4321-2017, 2017.

Harteg, J.: tipmip-gwl: global-warming-level coordinate mapping for TIPMIP, https://doi.org/10.5281/zenodo.23263429, version 1.1, 2026a.

Harteg, J.: tipmip-gwl: global-warming-level coordinate mapping for TIPMIP, https://doi.org/10.5281/zenodo.22084351, concept DOI, all versions, 2026b.

Jones, C., Bossert, I., Dennis, D. P., Jeffery, H. A., Jones, C. D., Koenigk, T., Loriani, S., Sanderson, B., Séférian, R., Wyser, K., Yang, S., Abe, M., Bathiany, S., Braconnot, P., Brovkin, V., Burger, F. A., Cadule, P., Castruccio, F. S., Danabasoglu, G., Dittus, A., Donges, J. F., Fröb, F., Frölicher, T. L., Georgievski, G., Guo, C., Hu, A., Lawrence, P., Lerner, P., Licón-Saláiz, J., Otto-Bliesner, B., Romanou, A., Shevliakova, E., Silvy, Y., Swingedouw, D., Tjiputra, J., Walton, J., Wiltshire, A., Winkelmann, R., Wood, R., Yokohata, T., and Ziehn, T.: The TIPMIP Earth system model experiment protocol: phase 1, Geoscientific Model Development, 19, 6941–6966, https://doi.org/10.5194/gmd-19-6941-2026, 2026.

Jones, C. D., Frölicher, T. L., Koven, C., MacDougall, A. H., Matthews, H. D., Zickfeld, K., Rogelj, J., Tokarska, K. B., Gillett, N. P., Ilyina, T., Meinshausen, M., Mengis, N., Séférian, R., Eby, M., and Burger, F. A.: The Zero Emissions Commitment Model Intercomparison Project (ZECMIP) contribution to C4MIP: quantifying committed climate changes following zero carbon emissions, Geoscientific Model Development, 12, 4375–4385, https://doi.org/10.5194/gmd-12-4375-2019, 2019.

Matthews, H. D., Gillett, N. P., Stott, P. A., and Zickfeld, K.: The proportionality of global warming to cumulative carbon emissions, Nature, 459, 829–832, https://doi.org/10.1038/nature08047, 2009.

Swaminathan, R., Parker, R. J., Jones, C. G., Allan, R. P., Quaife, T., Kelley, D. I., de Mora, L., and Walton, J.: The Physical Climate at Global Warming Thresholds as Seen in the U.K. Earth System Model, Journal of Climate, 35, 29–48, https://doi.org/10.1175/JCLI-D-21-0234.1, 2022.

Winkelmann, R., Dennis, D. P., Donges, J. F., Loriani, S., Klose, A. K., Abrams, J. F., Alvarez-Solas, J., Albrecht, T., Armstrong McKay, D., Bathiany, S., Blasco Navarro, J., Brovkin, V., Burke, E., Danabasoglu, G., Donner, R. V., Drüke, M., Georgievski, G., Goelzer, H., Harper, A. B., Hegerl, G., Hirota, M., Hu, A., Jackson, L. C., Jones, C., Kim, H., Koenigk, T., Lawrence, P., Lenton, T. M., Liddy, H., Licón-Saláiz, J., Menthon, M., Montoya, M., Nitzbon, J., Nowicki, S., Otto-Bliesner, B., Pausata, F., Rahmstorf, S., Ramin, K., Robinson, A., Rockström, J., Romanou, A., Sakschewski, B., Schädel, C., Sherwood, S., Smith, R. S., Steinert, N. J., Swingedouw, D., Willeit, M., Weijer, W., Wood, R., Wyser, K., and Yang, S.: The Tipping Points Modelling Intercomparison Project (TIPMIP): Assessing tipping point risks in the Earth system, EGUsphere, https://doi.org/10.5194/egusphere-2025-1899, preprint, 2025.

https://doi.org/10.5194/egusphere-2026-5162
Preprint. Discussion started: 12 November 2026
© Author(s) 2026. CC BY 4.0 License.

Appendix A: Baseline and monotonicity diagnostics

Table A1 lists, for each model, the branch year and pre-industrial reference adopted in Step 1, the drift of its `esm-piControl` run, and the maximum GWL its ramp-up reaches on the monotone axis. A trailing rather than centred baseline window is used for ACCESS-ESM1-5, EC-Earth3-ESM-1, GFDL-ESM2M, GISS-E2-1-G-CC2 and NorESM2-LM, whose branch years fall at the start of the staged `esm-piControl` record. Each mapping applies only to the ensemble member it was built from, since a different member branches from `esm-piControl` at its own point and follows its own warming trajectory.

Decoding alone is not sufficient for every model. For two models the branch year is absent from the published files and was supplied by the modelling group: UKESM1-2-LL (2277), which matches the value used in the TIPMIP protocol, and CESM2 (81).

For the three models marked ‡ in Table A1 the attribute is present, but refers to a spin-up parent or to a different time axis than the `esm-piControl`→`esm-up2p0` branch, so a naive decode returns a year that is not the branch point on the TIPMIP timeline. For GFDL-ESM2M, `branch_time_in_parent`=36500 is year 1961 of the `esm-piControl-spinup`, the hybrid restart state from which both `esm-piControl` and `esm-up2p0` were initialised; both child runs reset their time axis to 1861, which is therefore the branch year (confirmed by the modelling group). For GISS-E2-1-G-CC2, `branch_time_in_parent`=111690 is year 306 of a spin-up that is the shared parent of `esm-piControl` and `esm-up2p0` and was not submitted to TIPMIP; the two runs are year-aligned, so the branch from `esm-piControl` is its first year, 1850 (confirmed by the modelling group). For IPSL-CM6-ESMCO2, `branch_time_in_parent`=18250 is 50×365 days, but decoding it against the declared Gregorian parent calendar lands on 1849-12-20; the ramp-up runs parallel to `esm-piControl` from 1850, which is the branch year. In every case the adopted year and its provenance are recorded in the mapping product itself, as the `branch_year` and `branch_year_source` attributes.

https://doi.org/10.5194/egusphere-2026-5162
Preprint. Discussion started: 12 November 2026
© Author(s) 2026. CC BY 4.0 License.

Table A1. Per-model baseline and robustness diagnostics. The smaller grey line under each model name is the ensemble member (`variant_label`) the mapping was built from. Branch year: the year of `esm-piControl` from which the ramp-up branches; ‡ marks the three models whose branch year cannot be recovered by decoding `branch_time_in_parent` (see text). `esm-piControl` drift: linear trend of the full `esm-piControl` GMSAT (°C/century). `ref_full`: the full `esm-piControl` mean, reported as a diagnostic of each control record only (Sect. 2.3); not the adopted baseline. `ref_window`: the adopted baseline — the mean GMSAT over a 31-year window centred on the branch year, or over the first 31 years where the branch falls at the start of the control record. $|\Delta\mathrm{ref}|$: absolute difference between the two, at most 0.182 K across all models; reference means are given to 0.001 K to preserve this precision.

Model	Branch year	piControl range	Drift (°C cy^{-1})	Ref. full (K)	Ref. window (K)	$\lvert\Delta\mathrm{ref}\rvert$ (K)	Max GWL (°C)
IPSL-CM6-ESMCO2‡ r1i2p3f1	1850	1800–2449	-0.039	285.737	285.808	0.071	11.070
GISS-E2-1-G-CC2‡ r1i1p1f3	1850	1850–2299	-0.013	286.760	286.753	0.007	4.580
UKESM1-2-LL r1i1p1f1	2277	2100–2500	0.026	286.967	286.897	0.069	5.940
GFDL-ESM2M‡ r1i1p1f1	1861	1861–2521	0.018	286.978	286.796	0.182	4.100
CESM2 r1i1p1f1	81	1–714	0.014	287.254	287.242	0.012	4.220
NorESM2-LM r1i1p1f1	1851	1851–2310	0.007	287.611	287.602	0.009	4.250
ACCESS-ESM1-5 r1i1p1f1	271	271–770	0.023	287.724	287.673	0.051	4.230
EC-Earth3-ESM-1 r1i1p1f1	1850	1850–2450	-0.026	287.912	288.000	0.089	6.630
MIROC-ES2L r1i1p1f1	2001	1976–2475	-0.004	288.124	288.102	0.022	4.520

https://doi.org/10.5194/egusphere-2026-5162
Preprint. Discussion started: 12 November 2026
© Author(s) 2026. CC BY 4.0 License.

Table A2. Per-model maximum monotonicity adjustment (`mono_max`, °C) after the 31-yr centred running mean (edge-shortened where a full window is unavailable), for the ramp-up leg and the two ramp-down legs (from 2 °C and 4 °C holds). Computed as max|smoothed − monotone| on each leg's GWL axis (increasing PAVA on ramp-up; decreasing PAVA on ramp-down). Model order matches Table A1.

Model	Ramp-up	Ramp-down 2 °C	Ramp-down 4 °C
IPSL-CM6-ESMCO2	0.000	0.002	0.003
GISS-E2-1-G-CC2	0.003	0.001	0.004
UKESM1-2-LL	0.000	0.000	0.000
GFDL-ESM2M	0.001	0.000	0.001
CESM2	0.000	0.001	0.055
NorESM2-LM	0.001	0.000	0.007
ACCESS-ESM1-5	0.000	0.000	0.006
EC-Earth3-ESM-1	0.001	0.000	0.000
MIROC-ES2L	0.000	0.000	0.003